Kaersutite-bearing gabbroic inclusions and the late dike swarm of Kangerdlugssuaq, East Greenland

C. KENT BROOKS

Institute of Petrology, University of Copenhagen

R. G. PLATT

Grant Institute of Geology, University of Edinburgh[1]

SUMMARY. The Kangerdlugssuaq late dike swarm, which strikes at a high angle to the well-known East Greenland coastal swarm, is described and chemical analyses presented. The basic members are characterized by a high potassium content. A variety of kaersutite-bearing gabbroic inclusions in one member of this swarm is described in detail and microprobe analyses of clinopyroxenes, amphiboles, plagioclases, sheet silicates, and spinel minerals are presented. On the basis of this evidence it is deduced that these inclusions derive from a cumulate sequence formed at depths of between 5 and 10 km beneath the Lower Tertiary land surface. It is likely that fractionation of such assemblages causes a transition, at relatively low pressure, from undersaturated to oversaturated compositions, but the products appear to be quantitatively minor.

IN contrast to the well-known, coast-parallel dike swarm of East Greenland (Wager and Deer, 1938), there exists almost no information on the later, fjord-parallel swarm in Kangerdlugssuaq. In this paper we present petrological and chemical data on these rocks together with a detailed study of the minerals from an interesting suite of kaersutite-bearing plutonic inclusions in a member of the swarm.

Within the lower Tertiary igneous province of East Greenland (Brooks, 1973a and b), kaersutite-bearing dike rocks have earlier been described by Vincent (1953), while a dike containing kaersutite megacrysts, associated with sahlite and diopside megacrysts and ultramafic inclusions, all of high-pressure origin, has recently been described from Wiedemanns Fjord, 150 km to the east, by Brooks and Rucklidge (1973). The kaersutite inclusions described here are not likely to be of particularly high-pressure origin, as the assemblage of kaersutite, olivine, clinopyroxene, plagioclase, and Fe–Ti oxides is known to be unstable above relatively modest pressures (Yoder and Tilley, 1962; Ito and Kennedy, 1967). Similar inclusions have been described from Tristan da Cunha (LeMaitre, 1969), Gran Canaria (Frisch and Schmincke, 1969; Muñoz, 1973), Arizona and Nevada (Best, 1970), Japan (Aoki, 1970), Tenerife (Borley, Suddaby, and Scott, 1971), and Spain (Sagredo, 1973). All these occurrences are remarkably similar and all occur in alkali basalts and related rock types. In fact, all natural occurrences of kaersutite are in basic undersaturated rocks, although it has recently been demonstrated that this is more likely to be a consequence of higher volatile fugacities in magmas of this type compared to tholeiites, rather than any direct

[1] Present address: Dept. of Geology, Lakehead University, Thunder Bay, Ontario, Canada.

result of the undersaturation (Helz, 1973). The present occurrence is no exception to the general rule.

The present study has shown that the Kangerdlugssuaq late dike swarm belongs to a moderately potassic, strongly undersaturated suite. It is unusual in that the undersaturated nature of the basaltoid parents is not reflected in their differentiates, which in fact cross the critical plane of silica saturation of Yoder and Tilley (1962), apparently as a result of extensive kaersutite fractionation.

Geological setting

The late dike swarm (Wager, 1947, p. 40) trends roughly north–south parallel to Kangerdlugssuaq fjord (fig. 1) and cuts all other rocks of the district, including the alkaline Kangerdlugssuaq intrusion. Brooks (1973a) explained the area in terms of a lower Tertiary triple junction, with active ocean-floor spreading taking place only along the two arms parallel to the present coast and accompanied by intense tholeiitic magmatism and development of the well-known coastal dike swarm and flexure (Wager and Deer, 1938). Along the third arm now occupied by Kangerdlugssuaq, a rift-like structure developed, which did not spread, but which was the locus of alkaline magmatism. As such, it would be regarded by Burke and Dewey (1973) as a 'failed arm'. It is parallel to this structure that the late dike swarm trends.

The samples described here represent a small sample of the swarm taken in the area between Amdrups Fjord and Søndre Syenit Gletscher (fig. 1), where it cuts the syenites and nepheline syenites of the Kangerdlugssuaq intrusion (Kempe, Deer, and Wager, 1970) and the surrounding Precambrian gneisses. In general these dikes are not broad, the majority being of the order of a few metres in thickness. The fact that a few thicker ones, which are only found cutting the gneisses, tend to be extensively uralitized, suggests that older dikes may be present with the same trend. In particular the 50 m thick dike, which follows the west coast of the fjord and is depicted on the map of Wager (1947), belongs to this group. The inclusion-bearing dike (sample no. CKB70–50) cuts the basement but is little altered in spite of its proximity to the intrusion and is, therefore, believed to be contemporaneous with the dikes cutting the nearby plutonics.

Inclusions are not uncommon in these dikes, but are generally of gneiss or syenite. One example, in particular, was noted on the northern side of Amdrups Fjord that was crowded with rounded gneiss inclusions. Only one example with kaersutite gabbro inclusions is at present known, although there are indications in some of the other samples (e.g. CKB70–21) of small amounts of largely disintegrated inclusions of the same type. The general appearance of the kaersutite-gabbro-bearing dike at sea level in the small bay to the south of Søndre Syenit Gletscher is shown in fig. 2. However, where it outcrops higher up the hillside it has a thickness of 60 cm, but is quite free of inclusions. Here it is faintly banded, with a central vesicular zone. This suggests that the magma may have been extremely fluid, allowing settling of the inclusions over a distance of some 200 m before solidification of the thin dike, an observation supported by the common presence of very fine apophyses to many of these dikes. However, the distribution of xenoliths may alternatively be explained
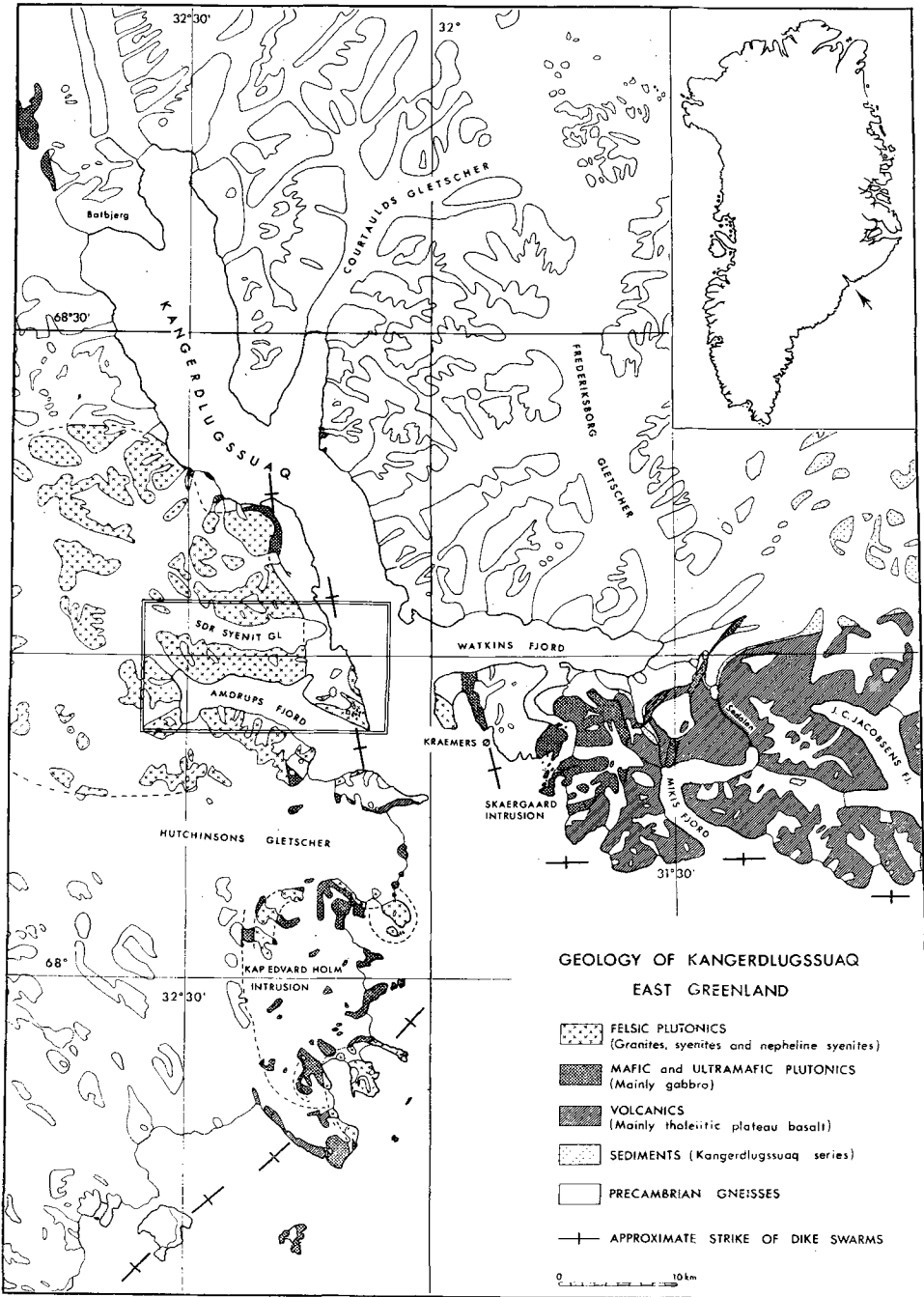
FIG. 1. Locality map. The area in which the dikes described here were collected is indicated by the rectangle.

in terms of intrusion dynamics as discussed by Bhattacharji and Smith (1964). In most cases the inclusions continue right up to the dike margins, but in some places the dike is bounded by an inclusion-free banded zone with up to ten bands of varying grain-size, suggestive either of multiple intrusion or flow differentiation.
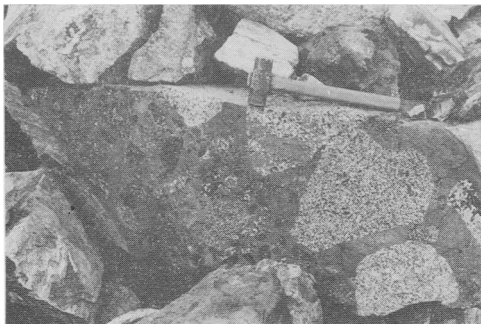

FIG. 2. A loose block detached from the inclusion-bearing dike (CKB70–50), showing the abundant inclusions of various types of kaersutite gabbros and clinopyroxene megacrysts. A fragment of the country rock (gneiss) may be seen at the left. The hammer is c. 35 cm long.

Petrology and chemistry of the late dike swarm

The rocks of the late dike swarm contrast strongly with those of the earlier, tholeiitic, coast-parallel swarm in the area (Vincent, 1950, 1953; Brooks, Nielsen, and Petersen, in prep.) in being distinctly alkaline. Analyses of a typical suite are reported in Table I, which also contains localities and brief petrographic descriptions. All (except CKB70–21)

Notes to Table I, opposite (ctd.).

are also present. The rock is an ankaramite and lies close to the critical plane of silica undersaturation, small adjustments in oxidation state being critical.

CKB70–26 Cuts foyaites on southerly nunatak at head of Sdr. Syenit Gl. Rich in phenocrysts, mainly clinopyroxene, up to 3 mm in size and unzoned, but also sparse, fresh olivines. A few xenocrysts of quartz are present, heavily embayed and rimmed. The groundmass is plagioclase, clinopyroxene, and ore (titanomagnetite and ilmenite). Small amounts of brown amphibole and patches of calcite are also present.

CKB70–27 Same locality as previous. Almost aphyric with sparse microphenocrysts of clinopyroxene and pseudomorphed olivine. Groundmass: plagioclase, brown amphibole, clinopyroxene, and ore. Calcite occurs interstitially and in vugs. Similar to CKB70–50.

CKB70–32 Cuts pulaskites on N. side Cdr. Syenit Gl. An ankaramite, with tightly packed clino-pyroxenes and some pseudomorphed olivines up to ¾ cm in size. The pyroxenes are unzoned, but extensively altered along margins and a network of cracks. The groundmass cannot be resolved, but contains brown amphibole, two types of ore, and plagioclase. Ocelli occur, which are more leucocratic and contain green amphibole.

CKB70–49 Dike cutting block, foot of Sdr. Syenit Gl. Phenocrysts are fresh, unzoned clinopyroxenes up to 7 mm in size and serpentine pseudomorphs after olivine. Lath-like microphenocrysts of plagioclase are enclosed in a dark, fine-grained groundmass containing pseudomorphed olivine. This dike apparently represents two phases of injection with basement xenoliths in between (excluded from analysis).

CKB70–50 Inclusion-rich dike in bay just S. of snout of Sdr. Syenit Gl. The matrix consists of phenocrysts of clinopyroxene, olivine (pseudomorphed by chlorite and/or calcite), and brown amphibole, all a few mm in size. Groundmass is fine-grained, consisting of acicular brown amphibole, plagioclase, clinopyroxene, and ore. The texture is typical of lamprophyres, with euhedral ferromagnesian minerals. Patches of calcite and chlorite occur sporadically.

NM5079 Cuts pulaskites at head of Amdrups Fjord and is notable for its cherry-red phenocrysts, which under the microscope are seen to be fresh olivine with minute films of oxidized material along cracks (cf. Kapp, 1960, p. 153 for reference to similar material from Mesters Vig area). These olivines are euhedral and up to 3 mm across. Zoned or corroded clinopyroxene also occurs as a phenocryst phase, but is less abundant. The dirty groundmass contains sparse plagioclase laths, clinopyroxene, brown amphibole, ore, etc.

TABLE I. *Analyses of rocks from the Kangerdlugssuaq late dike swarm*

	CKB 70–5	CKB 70–21	CKB 70–22	CKB 70–26	CKB 70–27	CKB 70–32	CKB 70–49	CKB 70–50	NM 5079
SiO_2	44·11	42·45	48·53	44·72	42·38	43·74	45·22	42·91	43·25
Al_2O_3	16·35	14·24	8·23	11·91	14·38	5·24	13·33	13·92	11·05
Fe_2O_3	3·79	4·19	2·86	2·87	5·31	1·34	2·06	4·57	2·25
FeO	5·05	4·68	6·63	7·09	5·02	6·28	6·78	5·96	7·00
MgO	7·1	5·22	12·45	7·0	5·8	13·3	7·6	9·0	13·92
CaO	10·71	11·21	14·12	9·91	10·45	13·36	8·78	10·89	11·33
Na_2O	2·83	4·71	1·71	2·98	3·39	1·54	3·80	2·60	1·34
K_2O	1·41	2·86	1·32	1·39	2·06	1·97	0·66	2·16	1·86
MnO	0·15	0·19	0·14	0·17	0·17	0·16	0·22	0·18	0·18
TiO_2	2·03	2·00	2·29	2·56	2·71	1·78	1·71	2·70	1·49
P_2O_5	0·73	1·35	0·74	0·55	0·70	0·58	0·50	0·65	0·40
CO_2	3·0	—	—	8·15	5·15	7·5	5·6	0·5	—
H_2O^+	2·50	—	—	0·46	1·56	1·80	2·9	2·5	—
H_2O^-	—	0·16	0·12	—	—	—	—	—	0·12
Loss on ignition	—	6·73	0·62	—	—	—	—	—	5·90
Total	99·76	99·99	99·76	99·76	99·08	98·59	99·16	98·54	100·09

C.I.P.W. weight norm (after recalculation to 100 % volatile-free and adjustment of Fe_2O_3/FeO ratio to 0·15)

or	8·81	18·14	7·86	8·98	13·18	13·06	4·31	13·36	11·70
ab	16·44	0·23	13·74	22·93	9·27	2·24	29·66	4·81	2·74
an	29·48	9·94	10·98	16·50	19·43	1·77	19·15	20·87	19·84
ne	4·85	23·07	0·49	2·57	11·80	6·67	3·14	9·86	5·03
di	17·75	33·06	43·97	27·30	25·98	54·38	20·54	25·29	29·72
ol	14·78	6·05	14·88	13·81	10·56	14·98	16·40	16·48	25·04
mt	1·72	1·74	1·78	2·03	2·03	1·61	1·82	2·02	1·84
il	4·08	4·08	4·39	5·34	5·56	3·78	3·59	5·37	3·00
ap	1·78	3·36	1·74	1·39	1·76	1·51	1·29	1·58	1·00
Phenocrysts	cpx+ol +plag	amph+ cpx+ap	cpx+ol (qtz)	cpx+ol (qtz)	cpx+ol	cpx+ol	cpx+ol +plag	cpx+ol +amph	cpx+ol

Analysts: CKB70–21, –22 and NM5079, J. Bailey (Institute of Petrology, Copenhagen University); all others, Ib Sørensen (Geological Survey of Greenland), determined on powders dried at 110 °C.

CKB70–5 N. side of Søndre Syenit Gletscher. Phenocrysts: pseudomorphed olivine (*c.* 3 mm in size), clinopyroxene and abundant plagioclase. Groundmass consists of olivine (pseudomorphed), clinopyroxene, plagioclase, and brown amphibole. Patches of calcite present.

CKB70–21 Low col between Sdr. Syenit Gl. and Amdrups Fjord. Has a blotchy appearance in hand specimen due to round dark blebs *c.* ¾ cm across in a light matrix. A large pyroxene cluster and a small syenitic inclusion (excluded from the analysis) are visible in hand specimen. Phenocrysts of brown amphibole (often with a core of different composition), clinopyroxene, with striking bright green cores and colourless rims, and apatite, all *c.* 2 mm in size, are present. The groundmass consists of euhedral amphibole, clinopyroxene, amphibole, ore, and apatite in a matrix of feldspathoids. The light matrix between the blebs is enriched in feldspathoid and calcite (note high loss on ignition).

CKB70–22 Cuts pulaskites on N. side of Sdr. Syenit Gl. Phenocrysts: abundant clinopyroxenes up to 1 cm in size, which are unzoned except for a thin rim. Olivines of similar size, but much sparser and surrounded by thick reaction rims. Groundmass: fine-grained, largely clinopyroxene, plagioclase, and ore with carbonate (after olivine?). Small amounts of brown amphibole and zeolites

contain phenocrysts of olivine and clinopyroxene. Two examples have large amounts of clinopyroxene phenocrysts and are doubtless accumulative types—they are best termed ankaramites. Other phenocryst phases may be plagioclase and brown amphibole and, in the one relatively differentiated type (CKB70–21), apatite. The groundmass generally consists of plagioclase, brown amphibole, olivine, ore, and calcite, but is frequently difficult to resolve. Ocelli are sometimes found and two examples contain sparse, highly corroded quartz grains, which may be xenocrysts or may have precipitated from the magma at high pressure, although this, on thermodynamic grounds (Bacon and Carmichael, 1973, p. 19), seems unlikely. The volatile-rich nature of these magmas is suggested by their frequently vesicular nature and their content of CO_2, which occurs as calcite filling the vesicles, replacing olivine, or as a finely divided constituent of the groundmass. Dike rocks of this nature with abundant ferromagnesian phenocrysts and much brown hornblende are commonly called lamprophyres. Some quartz-normative types also occur, but these are subordinate in number and will be discussed below.

In calculating the norms, it has been assumed that CO_2 was added as such, rather than as calcite. The oxidation ratios have also been converted to a fixed value of $Fe_2O_3/FeO = 0.15$, based on an approximate value generally found for oceanic tholeiite fresh glass. This probably represents a minimum value for these more alkaline rocks, but only in one case (CKB70–22) does non-application of this correction give rise to a small amount of hypersthene (1.8 %) in the norm. There is, therefore, little doubt that these rocks represent a late phase of alkaline (nepheline–olivine normative) basic magmatism in the area.

Very similar dike rocks have been reported from the area north of Scoresby Sund by Bearth (1959) and Kapp (1960), where alkaline plutonics, including nepheline syenites, also occur. Comparisons with other occurrences of amphibole-bearing inclusions, as noted in the introduction, shows that the host rocks tend to be very similar, namely alkali basalts to basanites. In particular, the close similarity between certain of these dikes (e.g. CKB70–27 and CKB70–50, the inclusion dike) and the lavas of Tristan da Cunha (Baker, Gass, Harris, and LeMaitre, 1964), especially the analysed olivine basalt (sample no. 6), should be mentioned. This is interesting, in view of the fact that inclusions of similar type occur in the Tristan volcanics (Le Maitre, 1969).

The analysis of the inclusion-bearing dike (CKB70–50) was carried out on matrix material sawn from a large xenolith-rich block. Chemically, it is clearly similar to the other samples, being relatively rich in normative nepheline and olivine and with a fairly high K_2O content for such a basic rock. It differs from most of the others in that it has amphibole as a phenocryst phase (although it is not impossible that this amphibole derives from the abundant amphibole-rich inclusions) and, therefore, resembles most closely the camptonites described by Vincent (1953) from the Skaergaard area c. 20 km to the south-east. However, its chemistry shows important differences and there is no evidence in this area for derivation from a tholeiitic parent (as suggested by Vincent for the Skaergaard dikes). This rock, under the microscope, shows close similarity to the host rock of the nodule-megacryst assemblage from

Wiedemanns Fjord, described by Brooks and Rucklidge (1973), for which no analysis was presented. Apart from the presence of amphibole phenocrysts, it closely resembles CKB70–27 both petrographically and chemically, suggesting that these phenocrysts may be related to the nature of the volatiles, the latter rock having a much higher CO_2/H_2O ratio.

Petrology of the kaersutite-bearing inclusions

The inclusions are subrounded to angular, fairly tightly packed in the matrix of the host rock, and up to 40 cm in size (see fig. 2). They vary from leucocratic types, rich
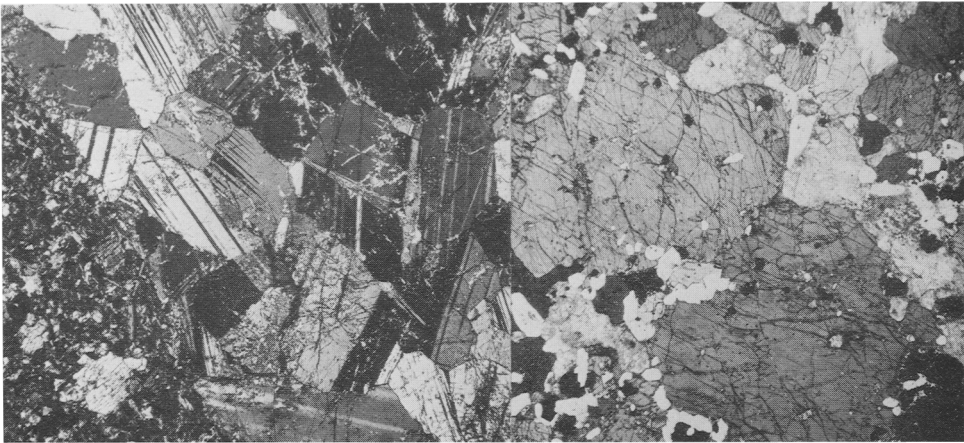
FIGS. 3 and 4: FIG. 3 (left). Inclusion of plagioclase cumulate in CKB70–50 in which the plagioclase has been enlarged by adcumulus growth to give an anorthosite. The host lamprophyre is seen at the lower left. The field of view is 4 mm. FIG. 4 (right). Apatite-rich kaersutite gabbro inclusion in CKB70–50. The rock has plagioclase, kaersutite, clinopyroxene, apatite, and ore as cumulus phases although the cumulate texture has been lost due to adcumulus growth. Field of view is c. 1 cm.

in plagioclase, sometimes monomineralic (fig. 3), sometimes with intercumulus, poikilitic amphibole, and clinopyroxene, to types composed almost entirely of amphibole and clinopyroxene. Striking cumulus textures are commonly developed and, in a few cases, lamination and suggestions of layering can be discerned. The grain-size is generally of the order of 0·5 cm, but some inclusions are much more coarse-grained, almost pegmatitic, with grains up to several cm in size. Support for the idea that the parent body was layered comes from the wide variation in modal composition of the inclusions, although they are largely composed of the same minerals.

The following five types have been subjected to detailed study, although the selection is not necessarily exhaustive or of any statistical significance: apatite-rich kaersutite gabbro (no. 1A/1)—abundant cumulus amphibole and apatite (fig. 4); kaersutite gabbro (no. 2A/1)—cumulus amphibole; olivine gabbro (nos. 1B/1 and 2A/2)—cumulus olivine (now pseudomorphed), clinopyroxene apparently intercumulus, with amphibole; anorthositic gabbro (no. 2B/1), composed largely of cumulus plagioclase

with some cumulus clinopyroxene, intercumulus amphibole, and clinopyroxene with a poikilitic texture; and brecciated pegmatitic gabbro (nos. 5 and 6)—completely disaggregated, but not dispersed; the individual crystals are often fragmented, and biotite is a notable constituent.

All the investigated types contain plagioclase as a cumulus phase, together with Fe–Ti oxides. The plagioclase is often partially sericitized and the titanomagnetite ($TiO_2 = c.$ 10 %) oxidized, with the exsolution of lamellae of ilmenite. Likewise, the ilmenite shows varying degrees of alteration to rutile and hematite. Olivine is always pseudomorphed and is restricted to a small number of the inclusions. The amphiboles carry exsolved plates of ilmenite, similar to that described by White (1966, p. 255) and Aoki (1970). Rounded blebs of sulphide occur within the amphiboles, a feature

TABLE II. *Modal compositions of amphibole gabbros from CKB70–50*

	1	2
Kaersutite	67·0	61·0
Plagioclase, in part altered	17·5	23·0
Clinopyroxene	0·5	8·5
Apatite	7·5	tr
Opaque minerals (oxides and sulphides)	5·0	6·0
Calcite–chlorite areas and alteration	2·5	1·5
Number of points counted	1455	1700

1. Apatite-rich kaersutite gabbro, xenolith 1A/1.
2. Kaersutite gabbro, xenolith 2A/1.

also noted by White (1966), in a manner suggesting that it may be derived from an immiscible melt. These sulphides include pyrite, pyrrhotine, pentlandite, chalcopyrite, cubanite, and chalcosine. Apatite is a ubiquitous and often abundant constituent. Biotite as a primary liquidus phase is restricted to the brecciated pegmatitic types, but occasionally occurs as a secondary phase in the other types.

Modes of the apatite-rich kaersutite gabbro and the kaersutite gabbro, the two most abundant types, are given in Table II.

Comparison with the petrology of kaersutite gabbro inclusions from other localities, as noted in the introduction, shows that many of these features are usual. Apart from the similarity of the host rocks mentioned already, both textures and mineral assemblages are similar to those described by other authors. This type of inclusion is characterized by cumulus textures, suggesting that it represents cognate material crystallized from the host rock at depth and contrasting strongly to the lherzolite and harzburgite inclusions, which show no signs of being cognate and do not have cumulus textures. The presence of large amounts of apatite seems to be a characteristic feature of many of these inclusions, e.g. Muñoz (1973) noted up to 8 % apatite in the inclusions of Gran Canaria. White (1966, p. 255) has described crusts of amphibole, biotite, and apatite round lherzolite nodules, which may well have been deposited under conditions similar to those under which the inclusions described here crystallized, while the nodules were undergoing transport to the surface. Orthopyroxene, not observed

in the Greenland material, is occasionally recorded as a minor constituent and is probably indicative of slightly greater depth of origin.

Mineralogy of the inclusions

Analytical method. The mineral analyses have been carried out by the second author on a Cambridge Instruments 'Microscan 5' microprobe at the University of Edinburgh, using an accelerating voltage of 15 kV and a current of 30 nA. Standards
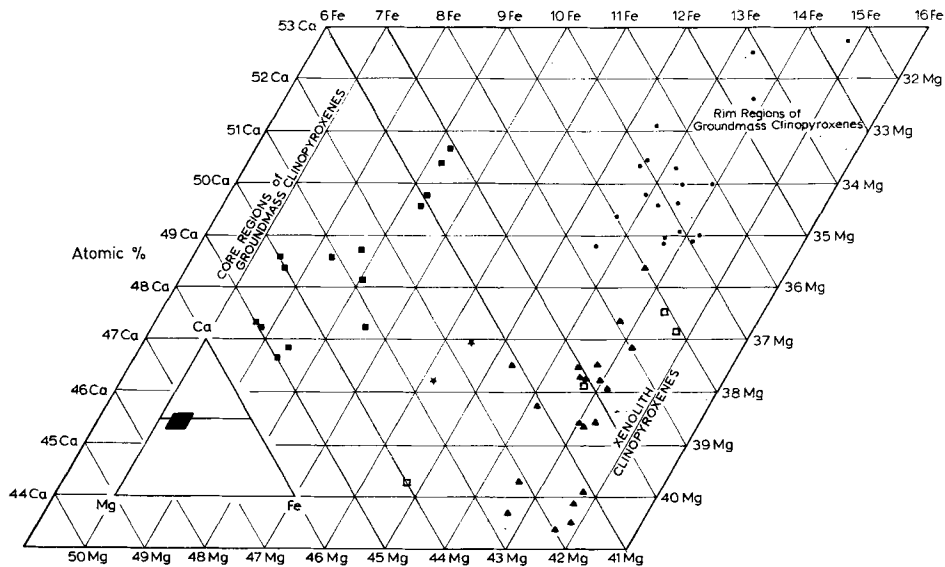

FIG. 5. Plot of individual clinopyroxene analyses from CKB70–50 with respect to Ca–Mg–Fe (atomic). Filled squares represent clinopyroxene phenocrysts, type (a), open squares those of type (b), triangles inclusion pyroxenes of type (b), stars clinopyroxene megacrysts, type (c), and filled circles groundmass and rim clinopyroxenes, type (d).

were simple oxides, silicates (wollastonite, orthoclase, jadeite), or metals and a full ZAF correction procedure was applied.

Clinopyroxenes. These are important constituents of all the sectioned inclusions and average analyses, representing 58 individual spot analyses, are reported in Table III. The complete data are plotted in figs. 5 and 6.

The cation proportions have been calculated on the basis of four metal ions instead of the usual six oxygens for the reasons given by Hamm and Vieten (1971) as this is more satisfactory for microprobe analyses. The proportions of the various clinopyroxene end-members have also been calculated as suggested by these authors and this has allowed an estimation of the relative amounts of Fe^{3+} and Fe^{2+}. Comparison with Fe^{3+} and Fe^{2+} estimated by assuming stoichiometry with respect to oxygen is good, but tests carried out on pyroxenes in which Fe_2O_3 and FeO have been determined chemically is not good. The significance of the calculated oxidation states and the

TABLE III. *Clinopyroxenes from the xenolithic lamprophyre (CKB70–50)*

	1	2	3	4	5	6	7	8	9	10
No. of analyses	2	4	4	2	3	4	14	2	19	2
SiO_2	47·46	48·64	48·37	49·54	52·88	51·86	49·29	52·19	44·72	48·37
Al_2O_3	6·47	5·67	6·02	4·81	1·79	2·26	5·91	1·44	9·27	6·33
Cr_2O_3	0·00	0·10	0·00	0·17	0·10	0·01	0·47	0·01	0·05	0·39
TiO_2	2·05	1·32	1·60	1·21	0·44	0·54	1·32	0·35	2·92	1·55
$FeO*$	8·01	7·93	8·30	7·78	8·57	8·91	5·15	8·95	7·68	6·79
MnO	0·17	0·18	0·17	0·15	0·54	0·35	0·10	0·67	0·14	0·13
MgO	12·65	13·31	13·15	14·01	13·76	14·05	14·45	13·07	11·72	13·84
CaO	21·91	21·20	21·45	20·98	21·46	20·62	22·63	22·65	22·32	21·31
Na_2O	0·59	0·61	0·60	0·58	0·49	0·57	0·43	0·63	0·51	0·48
Sum	99·31	98·96	99·66	99·23	100·03	99·17	99·75	99·16	99·33	99·19

Formula unit based on 4 cations†:

	1	2	3	4	5	6	7	8	9	10
Si	1·777	1·817	1·798	1·844	1·967	1·940	1·813	1·941	1·673	1·797
Al^{iv}	0·223	0·183	0·202	0·156	0·033	0·060	0·187	0·060	0·327	0·203
Al^{vi}	0·060	0·068	0·061	0·058	0·043	0·039	0·069	0·020	0·082	0·074
Cr	0·000	0·002	0·000	0·004	0·002	0·000	0·013	0·000	0·002	0·013
Fe^{3+}	0·087	0·082	0·096	0·068	0·070	0·051	0·061	0·067	0·113	0·068
Ti	0·058	0·038	0·045	0·033	0·011	0·016	0·037	0·009	0·083	0·042
Fe^{2+}	0·162	0·164	0·161	0·173	0·196	0·228	0·096	0·210	0·127	0·142
Mn	0·004	0·007	0·004	0·004	0·018	0·011	0·002	0·020	0·004	0·004
Mg	0·710	0·746	0·734	0·781	0·768	0·788	0·797	0·729	0·658	0·771
Ca	0·878	0·849	0·845	0·837	0·855	0·827	0·892	0·901	0·896	0·850
Na	0·040	0·045	0·045	0·040	0·036	0·040	0·030	0·045	0·036	0·036

Atom percent:

	1	2	3	4	5	6	7	8	9	10
Mg	38·65	40·52	39·98	42·01	40·06	41·61	43·17	38·12	36·68	42·11
Fe	13·55	13·36	14·00	12·96	14·08	14·73	8·50	14·53	13·38	11·47
Ca	47·79	46·12	46·02	45·02	45·26	43·66	48·32	47·25	49·94	46·42
100 Fe/ (Fe+Mg)	25·96	24·80	25·93	23·58	25·72	26·14	16·45	27·60	26·73	21·40

Theoretical pyroxene end-members after Kushiro (1962):

	1	2	3	4	5	6	7	8	9	10
$CaAl_2SiO_6$	6·0	7·0	6·1	6·2	4·6	3·9	8·2	2·0	8·4	8·7
$CaTiAl_2O_6$	5·8	3·8	4·5	3·3	1·1	1·6	3·7	0·9	8·3	4·2
$NaFeSi_2O_6$	4·0	4·5	4·5	4·0	3·7	4·0	3·0	4·5	3·6	3·6
$CaFeAlSiO_6$	4·7	3·7	5·1	2·8	0·0	0·0	3·1	2·2	7·7	3·2
$Mg_2Si_2O_6$	35·7	37·6	37·2	39·3	40·0	40·1	40·0	37·4	33·1	38·7
$Fe_2Si_2O_6$	8·1	8·2	8·0	8·7	10·0	11·5	4·8	10·5	6·3	7·1
$Ca_2Si_2O_6$	35·7	35·2	34·7	35·7	40·7	38·8	37·1	42·5	32·6	35·5

* Total iron as FeO.
† Fe^{3+}, Fe^{2+} determined from partitioning into the end-members as shown.

1. Apatite-rich kaersutite gabbro, xenolith 1A/1.
2. Altered olivine gabbro, xenolith 1B/1.
3. Kaersutite gabbro, xenolith 2A/1.
4. Altered olivine gabbro, xenolith 2A/2.
5. Intercumulus pyroxene in anorthositic gabbro, xenolith 2B/1.
6. Brecciated pegmatitic gabbro, xenolith 5.
7. Cores of phenocrysts in matrix, Cr-rich type.
8. Cores of phenocrysts in matrix, Cr-poor type.
9. Rims of phenocrysts in matrix.
10. Clinopyroxene megacryst, 1A/MCl.

amounts of the various clinopyroxene end-members should not be over-emphasized. Finger (1972) has discussed the problem of Fe_2O_3 estimation from microprobe analyses.

These clinopyroxenes fall into four main groups, which are seen clearly on the Ca–Mg–Fe plot in fig. 5 and correspond to four petrological types: *a*, certain clinopyroxene phenocrysts of the matrix; *b*, clinopyroxenes of the inclusions and those
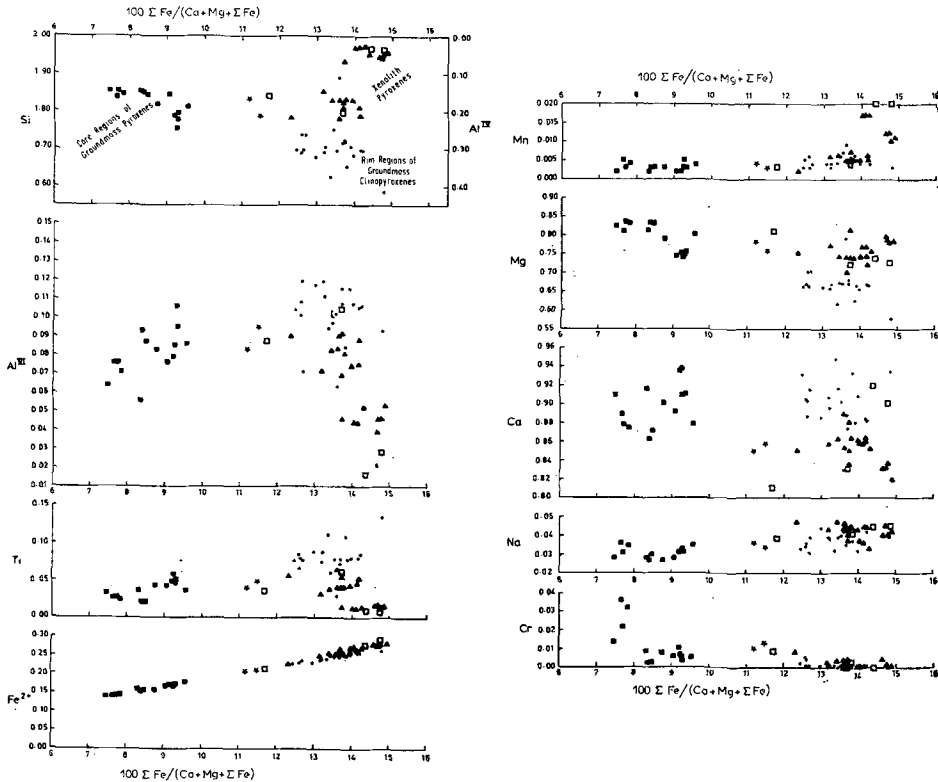

FIG. 6. Variation diagrams of the individual clinopyroxene analyses from CKB70–50. The symbols are the same as in the previous figure and correspond to the various clinopyroxene types discussed in the text.

phenocrysts that are not of type *a*; *c*, clinopyroxene megacrysts; and *d*, groundmass and rim clinopyroxenes. These various types are also distinguishable by their contents of minor elements (fig. 6) and subsidiary end-member molecules.

Briefly, the type *a* pyroxenes are rich in Mg, Cr, and Al^{vi}, they appear to be of relatively high-pressure origin and are reminiscent of the high-pressure relict paragenesis found in the Eifel ankaramites by Huckenholz (1966). In contrast, the type *b* pyroxenes are much richer in Fe and poorer in Cr and Al^{vi}; they have clearly crystallized under lower-pressure conditions. The megacrysts occupy an intermediate position,

while the type d pyroxenes (groundmass) are richer in Ca and Ti although having approximately the same Fe/Mg ratio as the inclusion pyroxenes.

In calculation of the theoretical molecules, Cr has been combined with Al, which, in effect, assumes that it is present as the $CaCrAlSiO_6$ (calcium-chromium Tschermak's) molecule. In fact, its presence as cosmochlore ($NaCrSi_2O_6$) is a possibility. Cr_2O_3 is below the detection limit in many of the inclusion pyroxenes (average 0·05 %), but reaches 0·47 % in the type a phenocrysts, which are chromium diopsides.

TiO_2 is relatively low in the type a phenocrysts (1·32 %) and the inclusions (1·19 %), but is high (2·92 %) in the rims of type d. This reflects the presence of the titanaugite component ($CaTiAl_2O_6$), which Yagi and Onuma (1967) have shown to decrease with increasing pressure and increase with differentiation.

Al^{vi} is generally regarded as being present in the form of Ca Tschermak's molecule ($CaAl_2SiO_6$), which increases with increasing pressure at the expense of anorthite (Kushiro, 1969). The inclusion pyroxenes, with an average of 0·054 Al^{vi} or 5·6 % Ca-Tschermak's molecule (after the method of calculation used here), would therefore correspond to lower pressures than those of the type a phenocrysts, which have 8·2 % $CaAl_2SiO_6$ (= 0·069 Al^{vi}). However, the rim and groundmass pyroxenes (type d) have 0·082 Al^{vi} or 8·4 % $CaAl_2SiO_6$ and this is not consistent with their obvious low-pressure paragenesis. This either reflects shortcomings in the calculation procedure or is the result of metastable incorporation of this component under conditions of rapid cooling, as suggested by Thompson (1972) for Vesuvian and lunar pyroxenes.

Muñoz and Sagredo (1974) have recently confirmed that the method of Aoki (1970) may be used as a geobarometer. They assigned pyroxenes from the Canary Islands to different depths on the basis of their content of minor components and, among other things, showed that the amphibole-bearing inclusions were derived from moderate depths. The Kangerdlugssuaq groundmass clinopyroxenes would, in spite of their high amounts of Ca-Tschermak's molecule, plot in Aoki's low-pressure field due to their high contents of the low-pressure components, $CaTiAl_2O_6$ and $CaFe^{3+}AlSiO_6$. On the basis of their Al^{vi} content, the megacrysts, type c, have also crystallized under appreciable pressure.

If any confidence can be placed in the calculated Fe^{3+} contents, a significant difference exists between the type a phenocrysts and the type b inclusion pyroxenes (Fe^{3+} = 0·061 and 0·076, respectively) and the type d rim and groundmass pyroxenes (Fe^{3+} = 0·113). This may reflect near-surface oxidation.

Variations in the pyroxene compositions from one inclusion to another are very small and it is probable that a great many more would have to be investigated before unambiguous relationships could be established. According to the differentiation index—$\Sigma Fe/(\Sigma Fe + Mn + Mg + Ca) \times 100$—and assuming that the inclusions represent a comagmatic sequence, the following differentiation sequence can be established: 1, altered olivine gabbro (2A/2, differentiation index = 12); 2, altered olivine gabbro (1B/1, diff. index = 13·3); 3, apatite-rich kaersutite gabbro (1A/1, diff. index = 13·5); 4, kaersutite gabbro (2A/1, diff. index = 14·0); 5, brecciated pegmatitic gabbro (5, diff. index 14·6). The anorthositic gabbro (2B/1) has not been placed in

this series as its clinopyroxene, at least in part, is intercumulus and, therefore, would come anomalously late in the series. This tentative sequence is difficult to support by other observations as the amphibole is frequently poikilitic (intercumulus) and the feldspars may be strongly zoned. The feldspars, however, except for the kaersutite gabbro (2A/1), whose feldspar is too basic, fit the sequence well if the outermost rim of the brecciated pegmatitic gabbro plagioclase is taken. It is interesting that, on this basis, the brecciated pegmatitic gabbro is the most evolved of the inclusions and this explains the appearance of biotite as a new phase. The pyroxenes of this rock are relatively enriched in Mn, Fe^{2+}, and Si and poor in Cr, Ca, and Ti (suggesting that earlier crystallized kaersutite had led to a depletion of the residual liquid in this last element). It is clear that, on this basis, olivine was a constituent of the early crystallizing paragenesis, while biotite occurred only in the latest, and this is a similar sequence to that described from the similar lavas and inclusions of Tristan da Cunha (Baker et al., 1964; LeMaitre, 1969).

If these pyroxenes are compared with earlier pyroxene analyses from similar rock types of the area we find that the lamprophyric phenocryst pyroxene analysed by Vincent (1953) falls in the field of the inclusion pyroxenes analysed in this study. The pyroxenes from the lamprophyre dike described by Brooks and Rucklidge (1973) have much more extreme compositions, the megacrysts being much more Mg-rich, the green 'phenocrysts' much more Fe-rich and the rims much richer in Ti, although occupying a similar position with respect to their Fe/(Fe+Mg) ratios to the rim pyroxenes described here, as would be expected if the host rock has similar composition.

In summary, it would appear that the type b inclusion pyroxenes and the type a phenocryst pyroxenes represent assemblages crystallized under different conditions of pressure, with the inclusion pyroxenes as the lower-pressure ones. The contrast in composition between the inclusion pyroxenes and the type d rim pyroxenes suggests that the inclusion pyroxenes have crystallized at higher pressure. The megacrysts represent an intermediate case between the inclusions and the type a phenocrysts and form a link between the two. Also present are the type b phenocrysts, which are similar to those of the inclusions. On the basis of close similarities to the supposedly most-differentiated inclusion types, it is suggested that they represent primocrysts, which were present in the magma chamber at the time of fragmentation of the underlying cumulates.

The problem of the depths of crystallization of these pyroxenes is discussed below.

Amphiboles are also ubiquitous and characteristic constituents of all inclusions. Average compositions, derived from a total of 23 spot analyses (all of which satisfy the criteria for superior analyses, as set out by Leake, 1968) are reported in Table IV.

The most striking feature of these amphiboles is their small range in compositions. Most fulfil the definition of kaersutite, while those that fall outside the kaersutite range, and should strictly be called titaniferous pargasites (Leake, 1968), do so only marginally and it does not seem reasonable to give them a different name. They are, therefore, all regarded as kaersutites, as was done by Aoki (1970), when faced with the same problem.

The differentiation index varies only slightly among the analysed amphiboles,

TABLE IV. *Amphiboles from the xenolithic lamprophyre* (*CKB70–50*)

	1	2	3	4	5	6	7	8	9
No. of analyses	3	3	4	2	2	1	3	2	3
SiO_2	39·88	39·84	39·39	40·67	40·19	40·50	40·59	40·44	37·56
Al_2O_3	13·06	13·20	13·67	11·89	11·42	11·98	12·32	12·23	14·61
Fe_2O_3	3·98	5·22	4·19	11·76	6·12	9·86	1·77	6·47	11·05
TiO_2	5·21	4·87	5·27	4·45	5·65	4·35	4·96	4·93	5·50
FeO	8·07	6·34	7·63	1·39	7·09	3·57	10·29	6·05	1·56
MnO	0·16	0·12	0·13	0·16	0·29	0·29	0·13	0·19	0·17
MgO	12·43	13·02	12·45	12·99	12·20	12·35	12·80	12·83	11·54
CaO	11·74	11·82	11·73	11·21	11·07	11·20	11·44	11·26	12·29
Na_2O	2·50	2·18	2·31	2·29	2·82	2·53	2·44	2·61	2·32
K_2O	0·92	1·35	1·19	1·14	1·11	1·32	1·23	0·93	1·36
H_2O^+	(2·04)	(2·04)	(2·03)	(2·05)	(2·03)	(2·04)	(2·03)	(2·04)	(2·04)
Sum	99·99	100·00	99·99	100·00	99·99	99·99	100·00	ʾ99·98	100·00

Formula unit based on 22O,2OH, equivalent to ½ unit cell:

	1	2	3	4	5	6	7	8	9
Si	5·873	5·849	5·799	5·923	5·938	5·941	5·998	5·933	5·515
Al^{iv}	2·127	2·151	2·201	2·041	1·989	2·059	2·002	2·067	2·485
Al^{vi}	0·139	0·132	0·171	0·000	0·000	0·012	0·144	0·147	0·044
Fe^{3+}	0·441	0·576	0·464	1·289	0·679	1·089	0·196	0·714	1·222
Ti	0·577	0·537	0·583	0·487	0·629	0·480	0·551	0·544	0·607
Fe^{2+}	0·994	0·779	0·941	0·169	0·879	0·438	1·272	0·743	0·192
Mn	0·020	0·015	0·016	0·019	0·037	0·036	0·016	0·023	0·021
Mg	2·728	2·849	2·731	2·819	2·686	2·700	2·821	2·807	2·525
Ca	1·853	1·860	1·850	1·749	1·753	1·760	1·811	1·769	1·934
Na	0·714	0·621	0·659	0·647	0·811	0·720	0·702	0·744	0·662
K	0·175	0·252	0·223	0·212	0·219	0·247	0·233	0·174	0·256
$(OH)^-$	2·000	2·000	2·000	2·000	2·000	2·000	2·000	2·000	2·000
Z	8·000	8·000	8·000	7·964	7·927	8·000	8·000	8·000	8·000
Y	4·899	4·888	4·906	4·783	4·910	4·756	5·000	4·878	4·611
X	2·742	2·733	2·732	2·608	2·783	2·727	2·746	2·687	2·852
mg	0·652	0·676	0·658	0·656	0·627	0·633	0·655	0·655	0·638

All analyses are superior analyses as defined by Leake (1968).
mg = $Mg/(Fe^{3+}+Fe^{2+}+Mn+Mg)$ after Niggli.

  1. apatite-rich kaersutite gabbro, xenolith 1A/1. Kaersutite.
  2. Altered olivine gabbro, xenolith 1B/1. Kaersutite.
  3. Kaersutite gabbro, xenolith 2A/1. Kaersutite.
  4. Altered olivine gabbro, xenolith 2A/2. Titaniferous ferri-ferroan pargasite.
  5. Anorthositic gabbro, xenolith 2B/1. Kaersutite.
  6. Flow-structured feldspathic area round xenolith 3/2. Titaniferous ferri-ferroan pargasite.
  7. Brecciated gabbro pegmatite, xenolith 5. Kaersutite.
  8. Matrix amphibole, type 1. Kaersutite.
  9. Matrix amphibole, type 2. Ferri-kaersutite.

extreme values for mg ($= Mg/(Mg+Mn+\Sigma Fe)$, atomic) being 0·676 and 0·627. Once again, it is one of the altered olivine gabbros (1B/1) that is the most primitive, in spite of the fact that its amphibole is intercumulus. The most highly evolved is the analysis of amphibole in an area of strong feldspar alignment round inclusion 3/2, which is effectively groundmass amphibole. It appears likely that this structure arose during the sinking of the inclusion into the solidifying groundmass. Two types of amphibole are present as phenocrysts in the matrix, which differ from each other slightly, but significantly. It appears most likely that the composition in column 8 of Table IV (type 1) is derived from the inclusions, whereas the type 2 phenocrysts (col. 9, Table IV), which are slightly more evolved (lower mg) and more Si-poor, as well as being highly oxidized, are true phenocrysts. However, the difference is quite minor.

When compared to other kaersutite analyses from the area, the unity of those in Table IV is clearly seen. That analysed by Vincent (1953) from Skærgaard is distinctly less basic with mg = 0·607, while the megacryst from Wiedemanns Fjord reported by Brooks and Rucklidge (1973) is more basic (mg = 0·755). The Wiedemanns Fjord groundmass and rim amphiboles (mg = 0·661) fall inside the range of compositions reported here, thus lending additional support to the idea of the similarity of the host rocks in the two cases.

All the inclusion localities with amphibole mentioned previously contain a very similar amphibole and it is unlikely that amphibole is a very sensitive indicator of the conditions of crystallization. Best (1970) suggested that Al^{vi} and K contents might be indicators of pressure and on this basis the Kangerdlugssuaq amphiboles are of relatively shallow origin. Of the two localities described by Best, in Arizona and Nevada, it was the latter that he regarded as the lower-pressure paragenesis on a number of features, and it is this one that Kangerdlugssuaq resembles most closely. Al^{vi} is much lower than in the Wiedemanns Fjord megacryst (Brooks and Rucklidge, 1973) or the Skærgaard kaersutites (Vincent, 1953) but similar to those reported by Aoki (1970). However, it does not yet appear possible to make any quantitative estimates from this parameter.

The greatest variation shown by these amphiboles is in the degree of oxidation, and this is so large it is not to be explained as an artefact of the method of calculation. The amphiboles from the altered olivine gabbro (xenolith 2A/2), the flow-structured feldspathic area, and the matrix amphibole type 2 would all fall into the category of oxykaersutites of Aoki (1963), who showed that their high Fe^{3+} content is due to oxidation at the time of pressure drop caused by eruption (presumably in this case, emplacement as a dike at high levels).

Plagioclases. Compositions of plagioclases based on 40 spot analyses are reported in Table V and the complete analytical data is shown plotted in fig. 7. All these inclusion plagioclases with one exception are labradorite, the exception being by-townite. This type of composition is quite usual for plagioclases from this assemblage. Aoki (1970) drew a clear distinction between megacrysts, which are predominantly andesine, and the labradorite phenocrysts and labradorite-bytownites of kaersutite-bearing inclusions. The andesine megacrysts were believed to have crystallized at

depths of 30 to 60 km under anhydrous conditions and in association with highly aluminous pyroxene (Ca and Al preferentially incorporated into pyroxene as Ca-Tschermak's molecule). On the other hand, the labradorite-bytownites were ascribed to crystallization under hydrous conditions at depths of 25 to 30 km.

TABLE V. *Plagioclases from the xenolithic lamprophyre* (*CKB70–50*)

	1	2	3	4	5	6	7
No. of analyses	4	4	2	3	2	5	10
SiO_2	53·54	49·05	51·26	55·27	56·10	54·11	52·81
Al_2O_3	28·36	31·58	30·32	27·66	26·81	28·36	28·88
FeO*	0·35	0·43	0·31	0·33	0·34	0·47	0·49
MgO	0·04	0·07	0·07	—	—	0·06	—
CaO	11·45	15·27	13·35	10·47	9·53	11·01	11·95
Na_2O	4·59	2·68	3·49	5·13	5·47	4·80	4·17
K_2O	0·45	0·17	0·30	0·44	0·59	0·50	0·42
MnO	0·00	0·00	0·01	—	—	0·00	—
Sum	98·78	99·25	99·11	99·30	98·84	99·31	98·72

Formula unit based on 32 oxygens:

	1	2	3	4	5	6	7
Si	9·815	9·050	9·409	10·037	10·211	9·860	9·700
Al	6·130	6·873	6·559	5·923	5·753	6·091	6·253
Fe^{2+}	0·054	0·066	0·049	0·051	0·060	0·071	0·075
Mg	0·011	0·019	0·009	—	—	0·016	—
Ca	2·250	3·020	2·625	2·039	1·857	2·150	2·354
Na	1·631	0·959	1·244	1·804	1·929	1·696	1·485
K	0·105	0·040	0·071	0·102	0·138	0·117	0·099
Mn	0·000	0·000	0·001	—	—	0·000	—

Feldspar end-members:

	1	2	3	4	5	6	7
Ab	39·5	22·8	30·3	44·2	47·7	41·3	36·4
An	57·8	76·1	67·9	53·1	48·7	55·6	61·1
Or	2·7	1·1	1·8	2·6	3·6	3·0	2·6

* All iron as FeO.

1. Apatite-rich kaersutite gabbro, xenolith 1A/1.
2. Kaersutite gabbro, xenolith 2A/1.
3. Altered olivine gabbro, xenolith 2A/2.
4. Anorthositic gabbro, xenolith 2B/1.
5. Flow-structured feldspathic area round xenolith 3/2.
6. Brecciated gabbro pegmatite, xenolith 5.
7. Brecciated gabbro pegmatite, xenolith 6 (this feldspar grain is strongly and complexly zoned, cf. fig. 6).

In comparison to many similar occurrences, the plagioclases of Table V are rather sodic. For instance, those of the kaersutite-bearing inclusions described by Aoki (1970) were An_{65}–An_{82} and those of LeMaitre (1969) were An_{82} and An_{85}. The origin of this difference is not easily found as it may be due to different magmatic

compositions, different pressures of crystallization, or varying water contents. In general, the plagioclases exhibit a trend of differentiation compatible to that deduced earlier, but the An-rich nature of the kaersutite gabbro (no. 2A/1) is anomalous.
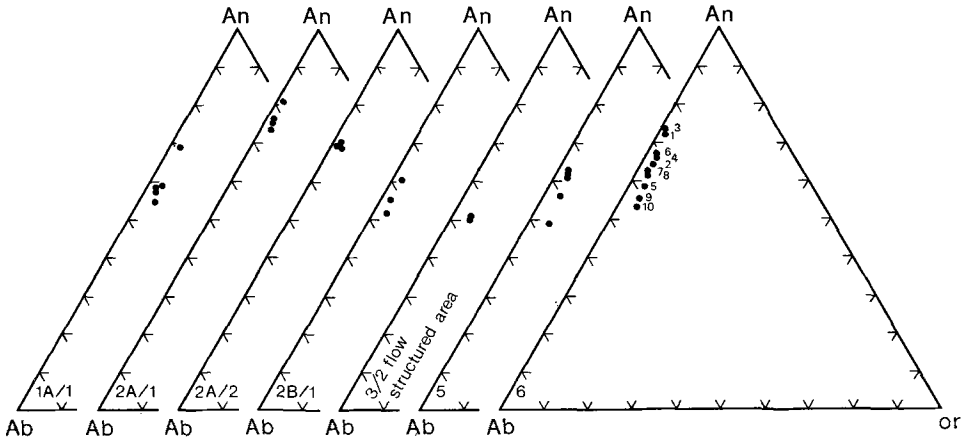

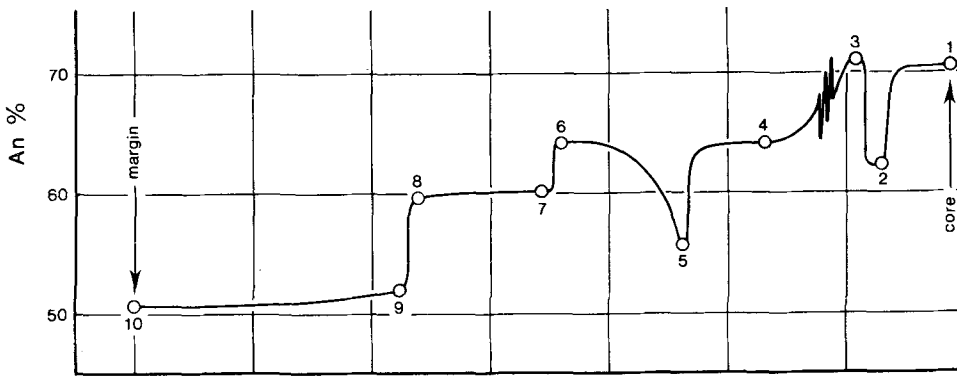FIG. 7. Compositions of plagioclases from the inclusions in CKB70–50.

FIG. 8. Profile showing the variation in An content of a zoned plagioclase in the brecciated pegmatitic gabbro (xenolith 6, CKB70–50). Compositions obtained by microprobe are shown as numbered circles. The distance from the core to the margin is c. 4 mm.

The most Ab-rich plagioclases come from the flow-structured groundmass area adjacent to inclusion 3/2, which also has one of the most Fe-rich amphiboles.

Plagioclase zoning is limited in all the investigated inclusions, except for the large grain of the brecciated pegmatitic gabbro (no. 6) where it is strong (fig. 8). This grain, which is c. 8 mm across, shows gradational and abrupt transitions together with both normal and reverse zoning; clearly the history of this grain has been extremely complex. Such complex zoning is also a feature of the plagioclases of layered intrusions, those of Skaergaard having been recently studied and interpreted by Maaløe

(1974). The presence of zoned plagioclase in the kaersutite gabbro inclusions of Gran Canaria was noted by Muñoz (1973) as a specific feature of this inclusion type.

Sheet silicates. Biotite occurring as a primary phase in the brecciated pegmatitic gabbros and as a secondary phase in the altered olivine gabbro (xenolith 2A/2) has been analysed and the compositions are shown in Table VI. These biotites resemble each other and have a composition falling in the high-Mg part of the biotite field of Deer, Howie, and Zussman (1962, p. 47), i.e. close to the phlogopite field. They are unusually rich in TiO_2, richer than any of the igneous biotites listed by Deer, Howie, and Zussman and this is presumably a reflection of correspondingly high TiO_2 in the

TABLE VI. *Sheet silicates from the xenolithic lamprophyre (CKB70–50)*

	I	2	3		I′	2′	3′
SiO_2	35·68	35·65	35·64	Si	5·351	5·365	6·135
Al_2O_3	14·41	14·40	16·17	Al	2·547	2·554	3·879
TiO_2	7·09	6·73	0·04	Ti	0·799	0·762	0·006
FeO*	13·60	12·73	17·50	Fe^{2+}	1·706	1·602	3·879
MnO	0·09	0·05	0·38	Mn	0·011	0·006	0·066
MgO	14·40	14·96	22·43	Mg	3·219	3·356	6·805
CaO	0·02	0·00	0·19	Ca	0·003	0·000	0·041
Na_2O	0·85	0·88	0·04	Na	0·248	0·257	0·016
K_2O	8·53	8·58	—	K	1·633	1·647	—
Cr_2O_3	—	—	0·00	Cr	—	—	0·000
Sum	94·67	93·98	92·39				

* Total Fe as FeO.

1. Average of four analyses of primary mica in brecciated pegmatitic gabbro, xenolith 5. Formula unit (I′) is based on 22 oxygens with H_2O^+ ignored.

2. Single analysis of secondary mica in altered olivine gabbro, xenolith 2A/2. Formula unit (2′) based on 22 oxygens with H_2O^+ ignored.

3. Single analysis of chlorite in calcite–chlorite-filled vug in matrix lamprophyre. Formula unit (3′) is based on 28 oxygens with H_2O^+ ignored.

magmas from which they crystallized. The presence of biotite in these particular inclusions is additional evidence for a high fugacity of water vapour and, taken in combination with the evidence from the coexisting minerals, suggests that this increased appreciably at a late stage when the brecciated pegmatitic gabbros were forming. This increase also apparently gave rise to the development of secondary biotite in the already-formed olivine gabbros. However, owing to the complicated relationships between biotites, water-vapour pressure, temperature, and oxygen fugacity (e.g. Eugster and Wones, 1958), it would be unwise to draw too deep-going conclusions from the presence of this mineral. Biotite is otherwise absent in the basic members of the Kangerdlugssuaq late dike swarm and it would not seem unreasonable to propose that the inclusions crystallized in a more water-rich environment than the dike rocks, which, as noted above, tend to be CO_2-rich.

Chlorite is a fairly common constituent of the matrix lamprophyre and the composition of such a chlorite, occurring in a vesicle with calcite, is also shown in Table VI. According to the classification of Hey (1954) it is a pycnochlorite.

Opaque oxides. Full analyses of three completely different spinel types are presented in Table VII. The analysis in col. 1 is a typical chromian spinel of the early stages of crystallization in basaltic magmas, a type that frequently occurs as inclusions in phenocrystic olivine, where it has been protected from subsequent reaction by the olivine (Thompson, 1973). The nature of the spinel from the megacryst is more problematical. Contrary to expectation, it does not closely resemble the spinels believed

TABLE VII. *Opaque oxides from the xenolithic lamprophyre (CKB70–50)*

	1	2	3	Formula unit based on 32 oxygens proportioned between $16R^{3+}$ and $8R^{2+}$		
	1	2	3		1	2	3
No. of analyses	4	2	2				
SiO_2	0·15	0·16	0·28				
TiO_2	1·58	5·30	8·81	Al	7·562	7·405	2·941
Al_2O_3	25·38	22·18	7·07	Cr	5·999	2·313	2·031
Cr_2O_3	30·01	10·33	7·27	Fe^{3+}	2·439	6·282	11·028
Fe_2O_3*	12·81	29·47	41·48	Fe^{2+}	2·716	3·441	5·247
FeO*	14·27	19·30	25·68	Mg	5·181	4·463	2·214
MgO	13·94	10·79	4·57	Mn	0·091	0·071	0·103
MnO	0·42	0·29	0·35	Ca	0·013	0·025	0·435
CaO	0·05	0·08	1·15				
Sum	98·61	97·90	96·66				

* Total Fe proportioned between Fe_2O_3 and FeO to generate the molecular ratio of RO/R_2O_3 of 1 (Stevens, 1944).

1. Spinel included within a serpentinized olivine phenocryst in the matrix. Chromian spinel.
2. Spinel included in clinopyroxene megacryst. Titaniferous ferrian spinel.
3. Exsolved spinel in clinopyroxene of kaersutite gabbro inclusion, xenolith 2A/1. Titaniferous aluminian magnetite.
(Nomenclature is based on Stevens, 1944.)

to be in equilibrium with the Wiedemanns Fjord megacrysts (Brooks and Rucklidge, 1973), but this may simply be because the latter are more basic. The spinel whose composition is reported in the third column (Table VII) occurs as short, stubby plates, which have apparently arisen by exsolution in two directions from the clinopyroxene host. They have a composition approaching magnetite.

The nomenclature adopted in the footnote to Table VII is the same as that of Stevens (1944) with the prefix 'titaniferous' added to indicate the appreciable contents of TiO_2 in spinels 2 and 3, a feature that cannot be taken into account on Stevens's triangular plot.

Discussion

Depth of crystallization. In the foregoing discussion much evidence has been brought forward relevant particularly to the depth of formation and, although an accurate

estimate is difficult, four factors relating to the conditions of crystallization may be summarized:

Octahedral Al in the clinopyroxenes of the inclusions suggests that the pressure was not high compared to typical lherzolite inclusions from alkali basalts or the mega-crysts from nearby Wiedemanns Fjord (Brooks and Rucklidge, 1973). The Cr-rich phenocrysts, however, stem from considerably greater depths.

Likewise, Al^{vi} and K in the amphiboles suggests relatively low pressure (cf. Best, 1970).

The coexistence of amphibole+clinopyroxene+plagioclase+olivine+mica simi-larly would be expected to be limited to relatively low pressures. Experimental data are not available for compositions close to that of the host rock, but the alkali basalt studied by Yoder and Tilley (1962, p. 452), one of the nearest compositions available, suggests that at $P_{H_2O} = P_{total}$ this assemblage is stable over a temperature range of c. 900–1000 °C and a pressure range of 0·5–3 kb. Above 3 kb plagioclase and pyroxene cease to coexist.

Estimates of the temperature of crystallization can be made from the Fe–Mg distribution between coexisting amphibole and clinopyroxene (Helz, 1973, p. 285). Values of this distribution coefficient (K_D) are: altered olivine gabbro (2A/2), $K_D = 1·68$; apatite-rich kaersutite gabbro (1A/1), $K_D = 1·50$; brecciated pegmatitic gabbro (5), $K_D = 1·47$. These partition coefficients indicate temperatures of 900 to 1000 °C, which is encouraging in that the various inclusions fall in the expected order, as deduced from paragenetic considerations, and coincide with the temperatures expected from Yoder and Tilley's (1962) experiments.

These considerations must be taken with considerable reservation owing to the differences in the compositions of the materials studied. In particular, amphibole in CKB70–50 is clearly, on textural evidence, a primary phase at low pressure, whereas in the sample studied by Yoder and Tilley (1962) it does not become so until c. 0·5 kb P_{H_2O}. All in all, however, it seems reasonable to conclude that a maximum depth of crystallization of about 10 km can be assumed. This is rather less than that suggested by LeMaitre (1969) for the similar inclusions of Tristan da Cunha, but similar to the conclusion of Muñoz and Sagredo (1974), who stated it must have been considerably less than 15 km for amphibole-bearing nodules of the Canary Islands.

A minimum depth of crystallization may be estimated from the field relationships. Wager (pers. comm., 1965) has estimated that about 3 km of basalts were originally present over this part of Kangerdlugssuaq and Kempe et al. (1970) assumed that the Kangerdlugssuaq intrusion crystallized under a pressure of c. 1 kb. It thus appears that 3 km is a reasonable minimum estimate, but it is perhaps surprising that, if these rocks crystallize at such limited depths, so few descriptions of kaersutite gabbros appear in the literature; most descriptions relate to inclusion suites.

Based on a variety of evidence, we therefore conclude that these gabbros originally crystallized at depths of between c. 5 and 10 km and at temperatures in the range 900 to 1000 °C. Using arguments similar to those of Muñoz and Sagredo (1974) depths of crystallization of around 20 km seem to be a reasonable rough estimate for the chromian diopside phenocrysts.

Effect of amphibole–pyroxene–plagioclase fractionation. Most authors who have studied this type of inclusion have come to the conclusion that they represent cognate cumulates of the host rock (e.g. LeMaitre, 1969; Aoki, 1970; Borley *et al.*, 1971; Sagredo, 1973; Muñoz, 1973), in contrast to the normal type of lherzolite inclusion, for which evidence has now crystallized in favour of an accidental origin in the upper mantle (e.g. Stueber and Ikramuddin, 1974). If this interpretation is correct, then it is reasonable to inquire what effect the crystallization of such an assemblage would have on the products. Cawthorn *et al.* (1973) showed convincingly that crystallization of amphibole from strongly undersaturated basic magmas in the Lesser Antilles led to

TABLE VIII. *Compositions and norms of typical amphibole and inclusion*

	I	2	C.I.P.W. weight norms		
				I	2
SiO_2	39·88	40·7	or	5·44	4·14
Al_2O_3	13·06	16·6	ab	0·66	4·72
Fe_2O_3	3·98	5·8	an	21·70	33·35
FeO	8·07	7·9	ne	11·10	7·53
MgO	12·43	9·0	di	28·75	23·80
CaO	11·74	12·8	ol	14·64	10·17
Na_2O	2·50	2·2	mt	5·77	8·41
K_2O	0·92	0·7	il	9·90	7·79
MnO	0·16	0·1			
TiO_2	5·21	4·1			
P_2O_5	—	—			
H_2O	2·04	—			
Total	99·99	99·9			

1. Kaersutite from inclusion 1A/1.
2. Calculated composition of inclusion 2A/1 (composition of ore taken as 67·8 % magnetite, 32·2 % ulvöspinel, corresponding to a titanomagnetite with 11·5 % TiO_2 as determined by probe).

a differentiation across the critical plane of silica undersaturation to give oversaturated products. Frisch and Schmincke (1969), on the other hand, invoked the suggestion of Bowen (1928) and ascribed the generation of the strongly alkaline Roque Nublo Series of Gran Canaria to resorption of early-formed kaersutite with the inclusions as residual material.

In Table VIII is shown the normative composition of a typical kaersutite and the calculated composition and norm of a typical inclusion. Both are strongly nepheline normative, although the great variability of the late dike swarm makes it perhaps more difficult to predict the effect of such fractionation than in the case of the lavas discussed by Cawthorn *et al.* (1973). Withdrawal of such compositions will undoubtedly drive many of the compositions given in Table I towards silica enrichment.

Apart from the basic dikes already described, a subordinate number of more differentiated types occur and these are in most cases (CKB70–21, Table I is an exception) oversaturated. Analyses of three of these dikes are presented in Table IX, where it

can be seen that up to 14 % normative quartz is encountered. Variation diagrams of the late dike swarm (Brooks, Nielsen, and Petersen, in preparation) give no evidence that the basic and differentiated members of this swarm are not cogenetic and we conclude that this trend has arisen by withdrawal of the assemblages described above, leading to a crossing of the thermal divide in the basalt system at relatively low

TABLE IX. *Compositions and norms of differentiated members of the late dike swarm, Kangerdlugssuaq*

	CKB 70–38	CKB 70–8	CKB 70–17		CKB 70–38	CKB 70–8	CKB 70–17
SiO_2	58·02	64·35	59·39	Q	11·50	13·95	5·12
Al_2O_3	17·06	16·21	17·05	or	13·89	22·58	17·02
Fe_2O_3	1·67	1·90	2·44	ab	32·83	40·62	47·90
FeO	3·03	2·42	4·32	an	24·19	11·73	13·16
MgO	2·90	1·50	1·80	di	4·46	1·44	2·51
CaO	5·98	3·02	3·71	hy	8·20	4·56	7·68
Na_2O	3·72	4·76	5·59	mt	2·52	2·77	3·58
K_2O	2·25	3·79	2·85	il	1·99	1·80	2·15
MnO	0·10	0·10	0·17	ap	0·42	0·56	0·86
TiO_2	1·01	0·94	1·12				
P_2O_5	0·17	0·24	0·37	Norms are calculated after			
H_2O^+	1·50	0·84	1·18	adjustment to 100%, H_2O and			
CO_2	2·20	—	—	CO_2 free.			
Total	99·61	100·07	99·99				

CKB70–38 N. side of Amdrups Fjord just beyond valley with waterfall. Phenocrysts are 3-mm plagioclases and altered ferromagnesians, probably originally largely biotite. The groundmass consists of feldspar, green amphibole, and ore. A little epidote and chlorite are present.

CKB70–8 Cuts Snout Series syenites, Amdrups Fjord. Phenocrysts of plagioclase rimmed by alkali feldspar are up to 3 mm in size and may be of xenocrystal origin. Smaller lath-shaped microphenocrysts of strongly zoned plagioclase, biotite, and titanomagnetite are set in a fine-grained groundmass of biotite, green amphibole (hornblende), feldspar, and ore. Epidote occurs in a vug.

CKB70–17 Cuts gneisses just S. of snout of Sdr. Syenit Gl. Occasional lath-shaped feldspar phenocrysts, up to 1 cm in length with a core of acid plagioclase rimmed by sericitized alkali feldspar. Groundmass is a fine-grained mixture of alkali feldspar, green amphibole (hornblende), and ore. A little quartz is also present.

pressure (equivalent to *c*. 5 to 10 km). The Tristan inclusions can also be shown to be fractionates that have led to the observed trend in the lavas, but in this case, oversaturated products do not seem to have been produced (LeMaitre, 1969).

Coombs and Wilkinson (1969) recognized a spectrum of lines of descent of the magmas of the East Otago province of New Zealand and elsewhere. The Kangerdlugssuaq late dike swarm closely resembles certain potassic lavas described by these authors, CKB70–50 being particularly close to certain nepheline basanites from Omini (Coombs and Wilkinson, 1969, Table 2), which belong to a strongly undersaturated, moderately potassic series. These authors noted that in many rocks of this type kaersutite is present and the differentiation trend is one of low Fe enrichment. The Kangerdlugssuaq rocks add yet another series to the many described by Coombs and

Wilkinson, who emphasized that in the series studied by them the degree of under-saturation of the basaltoid parents was reflected in the differentiates.

Intrusion and crystallization history. These inclusions are apparently not cognate with their matrix, as this contains clinopyroxene phenocrysts and megacrysts, which are almost certainly of a much greater depth of origin than the inclusions themselves. However, in view of the close petrographic similarity between the inclusions and the matrix, especially the similarity of the amphiboles, a close genetic relationship cannot be denied. It is therefore suggested that an undersaturated water-rich magma rose to a level of some 5 to 10 km in the crust and underwent prolonged fractionation to form a layered sequence of olivine–kaersutite gabbros through various types of kaersutite–clinopyroxene–plagioclase–apatite cumulates to coarse-grained pegmatitic biotite-bearing gabbros. The composition of the magma did not, however, change greatly in this time as the mineral compositions are relatively restricted. When the last-mentioned inclusion type was still incompletely consolidated, a new pulse of the same magma arrived from depth, brecciating the latest cumulates and disrupting the earlier ones into coherent blocks. The mixture of cumulate fragments, phenocrysts, megacrysts, and the surrounding liquid was subsequently swept upwards and intruded to form the dike sampled by us, in which a certain amount of settling took place before final solidification. These phases therefore are witness to crystallization at four different levels: the Cr-rich phenocrysts at depths of *c.* 20 km, i.e. near the base of the crust, the megacrysts at an intermediate level, the cumulates in a crustal magma chamber at 5 to 10 km, and finally the matrix under subvolcanic conditions, i.e. less than *c.* 5 km.

Regional implications. The late dike swarm in the area sampled represents an interesting undersaturated basic suite, which appears to be unusual in the Tertiary North Atlantic Province. In particular, the high potassium contents, relative to sodium, of many of the dike-rocks invites more detailed investigation and comparison with the well-known potassic provinces of the rift valleys.

The cognate suite of kaersutite-bearing gabbros are interesting in themselves, but do not, at first sight, appear to have had any quantitatively significant effect on the magmatic evolution of the area.

REFERENCES

AOKI (K.), 1963. The kaersutites and oxykaersutites from alkalic rocks of Japan and surrounding areas. *Journ. Petrology*, 4, 198–210.

—— 1970. Petrology of kaersutite-bearing ultramafic and mafic inclusions in Iki island, Japan. *Contr. Min. Petr.* 25, 270–83.

BACON (C. R.) and CARMICHAEL (I. S. E.), 1973. Stages in the P–T path of ascending basalt magma: an example from San Quintin, Baja California. Ibid. 41, 1–22.

BAKER (P. E.), GASS (I. G.), HARRIS (P. G.), and LEMAITRE (R. W.), 1964. The volcanological report of the Royal Society Expedition to Tristan da Cunha, 1962. *Phil. Trans. Roy. Soc., ser. A*, 256, 439–578.

BEARTH (P.), 1959. On the alkali massif of the Werner Bjerge in East Greenland. *Medd. Grønland*, **153** (4).

BEST (M. G.), 1970. Kaersutite-peridotite inclusions and kindred megacrysts in basanitic lavas, Grand Canyon, Arizona. *Contr. Min. Petr.* **27**, 25–44.

BHATTACHARJI (S.) and SMITH (C. H.), 1964. Flowage differentiation. *Science*, **145**, 150–3.

BORLEY (G. D.), SUDDABY (P.), and SCOTT (P.), 1971. Some xenoliths from the alkalic rocks of Teneriffe, Canary Islands. *Contr. Min. Petr.* **31**, 102–14.

BOWEN (N. L.), 1928. *The Evolution of the Igneous Rocks.* Princeton University Press.

BROOKS (C. K.), 1973a. Rifting and doming in southern East Greenland. *Nature Phys. Sci.* **244**, 23–5.

—— 1973b. The Tertiary of Greenland: a volcanic and plutonic record of continental break-up. *Amer. Assoc. Petroleum Geologists, Mem.* **19**, 150–60.

—— and RUCKLIDGE (J. C.), 1973. A Tertiary lamprophyre dike with high pressure xenoliths and megacrysts from Wiedemanns Fjord, East Greenland. *Contr. Min. Petr.* **42**, 197–212.

BURKE (K.) and DEWEY (J. F.), 1973. Plume generated triple junctions: key indicators in applying plate tectonics to old rocks. *Journ. Geol.* **81**, 406–33.

CAWTHORN (R. G.), CURRAN (E. B.), and ARCULUS (R. J.), 1973. A petrogenetic model for the origin of the calc-alkaline suite of Grenada, Lesser Antilles. *Journ. Petrology*, **14**, 327–37.

COOMBS (D. S.) and WILKINSON (J. F. G.), 1969. Lineages and fractionation trends in undersaturated volcanic rocks from the East Otago Province (New Zealand) and related rocks. Ibid. **10**, 440–501.

DEER (W. A.), HOWIE (R. A.), and ZUSSMAN (J.), 1962. *Rock-forming Minerals*, vol. 3. Sheet silicates. London (Longmans).

EUGSTER (H. P.) and WONES (D. R.), 1958. Phase relations of hydrous silicates with intermediate Fe/Mg ratios. *Carnegie Inst. Washington Year Book*, **57**, 193.

FINGER (L. W.), 1972. The uncertainty in the calculated ferric iron content of a microprobe analysis. Ibid. **71**, 600–3.

FRISCH (T.) and SCHMINCKE (H.-U.), 1969. Petrology of clinopyroxene-amphibole inclusions from the Roque Nublo volcanics, Gran Canaria, Canary Islands (Petrology of Roque Nublo volcanics I). *Bull. Volcanol.* **33**, 1073–88.

HAMM (H.-M.) and VIETEN (K.), 1971. Zur Berechnung der kristall-chemischen Formel und des Fe^{3+} Gehaltes von Klinopyroxen aus Elektronstrahl-Mikroanalysen. *Neues Jahrb. Min. Monatsh.* 310–14.

HELZ (R. T.), 1973. Phase relations of basalts in their melting range at $P_{H_2O} = 5$ kb as a function of oxygen fugacity. Part I. Mafic phases. *Journ. Petrology*, **14**, 249–302.

HEY (M. H.), 1954. A new review of the chlorites. *Min. Mag.* **30**, 277–92.

HUCKENHOLZ (H. G.), 1966. Der petrogenetische Werdegang der Klinopyroxene in der tertiären Vulkaniten der Hocheifel: III Die Klinopyroxene der Pikritbasalte. *Contr. Min. Petr.* **12**, 73–95.

ITO (K.) and KENNEDY (G. C.), 1967. Melting and phase relations in a natural peridotite to 40 kilobars. *Amer. Journ. Sci.* **265**, 519–38.

KAPP (H.), 1960. Zur Petrologie der Subvulkane zwischen Mesters Vig und Antarctic Havn (Ost-Grönland). *Medd. Grønland*, **153** (2).

KEMPE (D. C. R.), DEER (W. A.), and WAGER (L. R.), 1970. Geological investigations in East Greenland. Part VIII. The petrology of the Kangerdlugssuaq alkaline intrusion, East Greenland. Ibid. **190** (2).

KUSHIRO (I.), 1962. Clinopyroxene solid solutions. Part I. The $CaAl_2SiO_6$ component. *Japan Journ. Geol. Geogr.* **33**, 212–20.

—— 1969. Clinopyroxene solid solutions formed by reactions between diopside and plagioclase at high pressures. *Min. Soc. Amer. Spec. Paper*, **2**, 179–91.

LEAKE (B. E.), 1968. A catalogue of analysed calciferous and subcalciferous amphiboles together with their nomenclature and associated minerals. *Spec. Paper Geol. Soc. Amer.* 98.

LEMAITRE (R. W.), 1969. Kaersutite-bearing plutonic xenoliths from Tristan da Cunha, South Atlantic. *Min. Mag.* **37**, 185–97.

MAALØE (S.), 1974. *Zoned plagioclase of the Skaergaard intrusion, East Greenland.* Unpublished dissertation, University of Copenhagen.

MUÑOZ (M.), 1973. Inclusiones máficas y ultramáficas en las formaciones volcánicas de la isla de Gran Canaria. *Estudios Geologicos Inst. 'Lucas Mallada'*, **29**, 113–30.

—— and SAGREDO (J.), 1974. Clinopyroxenes as geobarometric indicators in mafic and ultramafic rocks from the Canary Islands. *Contr. Min. Petr.* **44**, 139–47.

SAGREDO (J.), 1973. Estudio de las enclaves de rocas ultramáficas con anfibol que aparecen en los basaltos al NW de Cartagena (provincia de Murcia). *Estudios Geologicos Inst. 'Lucas Mallada'*, **29**, 53–62.

STEVENS (R. E.), 1944. Composition of some chromites of the Western Hemisphere. *Amer. Min.* **29**, 1–34.

STUEBER (A. M.) and IKRAMUDDIN (M.), 1974. Rubidium, strontium and the isotopic composition of strontium in ultramafic nodule minerals and host basalts. *Geochimica Acta*, **38**, 207–16.

THOMPSON (R. N.), 1972. Oscillatory and sector zoning in augite from a Vesuvian lava. *Carnegie Inst. Washington Year Book* **71**, 463–70.

—— 1973. Titanian chromite and chromian titanomagnetite from a Snake River Plain basalt, a terrestrial analogue to lunar spinels. *Amer. Min.* **58**, 826–30.

VINCENT (E. A.), 1950. The chemical composition and physical properties of the residual glass of the Kap Daussy tholeiite dike, East Greenland. *Min. Mag.* **29**, 46–62.

—— 1953. Hornblende–lamprophyre dykes of basaltic parentage from the Skaergaard area, East Greenland. *Quart. Journ. Geol. Soc.* **109**, 21–50.

WAGER (L. R.), 1947. Geological investigations in East Greenland. Part IV. The stratigraphy and tectonics of Knud Rasmussens Land and the Kangerdlugssuaq region. *Medd. Grønland*, **105** (3).

—— and DEER (W. A.), 1938. A dyke swarm and crustal flexure in East Greenland. *Geol. Mag.* **75**, 39–46.

WHITE (R. W.), 1966. Ultramafic inclusions in basaltic rocks from Hawaii. *Contr. Min. Petr.* **12**, 245–314.

YAGI (K.) and ONUMA (K.), 1967. The join $CaMgSi_2O_6-CaTiAl_2O_6$ and its bearing on the titanaugites. *Journ. Fac. Sci. Hokaido Univ.* ser. 4, **13**, 463–83.

YODER (H. S.) and TILLEY (C. E.), 1962. Origin of basalt magmas: an experimental study of natural and synthetic rock systems. *Journ. Petrology*, **3**, 342–532.